

Exploring Spectral Index Band and Vegetation Indices for Estimating Vegetation Area

Iswari Nur Hidayati, R. Suharyadi and Projo Danoedoro

Received: 2018-06-03 / Revision: 2018-11-27 / Accepted: 2018-10-19
© 2018. Faculty of Geography UGM and The Indonesian Geographers Association

Abstract Visual analysis and transformation of vegetation indices have been widely applied in studies of vegetation density using remote sensing data. However, visual analysis is time intensive compared to index transformation. On the other hand, the index transformation from medium resolution imagery is not fully representative for urban vegetation studies. Meanwhile, the spectral range of high-resolution imagery is usually limited to visible wavelengths for the image transformation. Worldview-2 imagery provides a new breakthrough with a high spatial resolution and supports various spectral resolutions. This study aims to explore the spectral value of the Worldview-2 image index for estimation of vegetation density. Normalized indices were made for 56 band combinations and Otsu thresholding was implemented for the threshold selection to separate vegetation and non-vegetation areas. This thresholding was done by minimizing classes' variances between two groups of pixels which are distinguished by system or classification. The image binarization process was performed to differentiate between vegetation and non-vegetation. For the accuracy testing, a total of 250 samples was produced by a stratified random sampling method. Our results show that the combination of indices from red channel, red-edge, NIR-1, and NIR-2 provides the best accuracy for semantic accuracy. Vegetation area extracted from the index was then compared with the results of the visual analysis. Although the index results in area difference of 2.32 m² compared to visual analysis, the combination of NIR-2 and red bands can give an accuracy of 96.29 %.

Keywords: vegetation density, spectral index, normalized index

Abstrak Keberadaan vegetasi menjadi salah satu parameter terkait lingkungan perkotaan yang asri dan menarik. Vegetasi perkotaan juga menjadi penyeimbang ekologis perkotaan. Dalam kajian perkotaan dan penginderaan jauh, vegetasi menjadi objek yang sangat sering dikaji terkait dengan jumlah keberadaannya, jenis spesies, bahkan hingga kandungan biomassa dan kandungan oksigen di dalamnya. Kendala yang dihadapi dalam perhitungan kepadatan vegetasi adalah kepadatan bangunan, aksesibilitas, dan bercampurnya vegetasi dengan lahan terbuka. Penelitian kepadatan vegetasi menggunakan data penginderaan jauh biasanya menggunakan analisis visual dan transformasi indeks vegetasi. Analisis visual memerlukan waktu yang lebih lama jika dibandingkan dengan transformasi indeks. Keterbatasan pembuatan indeks untuk citra resolusi menengah adalah pada resolusi spasial citra yang masih belum representatif untuk penelitian vegetasi perkotaan. Sedangkan, citra resolusi tinggi masih terbatas pada panjang gelombang visible untuk pengolahan transformasi citra. Citra worldview-2 memberikan terobosan baru dengan resolusi spasial yang tinggi dan didukung resolusi spectral yang beragam. Penelitian ini bertujuan untuk eksplorasi nilai spectral indeks citra worldview untuk estimasi kepadatan vegetasi. Tahapan dimulai dari pembuatan normalized index untuk 56 kombinasi band. Pemilihan threshold untuk memisahkan area vegetasi dan non vegetasi menggunakan Otsu thresholding dengan meminimalkan varians dalam kelas dari dua kelompok piksel yang dibedakan oleh system/klasifikasi. Proses binarisasi citra digunakan untuk membedakan vegetasi dan non vegetasi yang selanjutnya dilakukan uji akurasi. Stratified random sampling menjadi metode untuk pengambilan sampel yang menghasilkan 250 sampel untuk uji akurasi. Kombinasi indeks dari saluran merah, red-edge, NIR-1, dan NIR-2 memberikan akurasi terbaik untuk akurasi semantic. Perhitungan kepadatan vegetasi pada indeks dibandingkan dengan hasil analisis visual citra. Walaupun hasil indeks mendapatkan luasan lebih rendah dibandingkan dengan analisis visual, kombinasi NIR-2 dan Red mempunyai akurasi tertinggi yaitu 96.29% dengan perbedaan luas 2.32 m².

Kata kunci: vegetasi, indeks spasial, normalisasi indeks

1. Introduction

In the scope of macro and micro development planning, vegetation has an important role in the ecosystem balance in urban areas. Urban biophysical

characteristics can be estimated and measured using several methods including field measurements, visualization and interpretation of aerial photographs and satellite imagery, and digital interpretation of remote sensing data. Field measurements and visualization of satellite image or aerial photo, both have been widely conducted and are still superior compared to other methods in term of accuracy (Duro et al., 2012). However, field measurement is a timely and costly activity. On the other hand, although visualization of satellite image and aerial photography have also been used for measurements of vegetation, canopy types,

and vegetation density, this process takes a long time when applied to a large area. Image visualization has a limitation since the digitization process and the data editing process requires synchronization and consistency in interpretation (Roy et al., 2015). Differences in perceptions of interpretation can also affect the mapping accuracy, thus an interpretation method is needed to calculate vegetation density quickly. The use of imagery is dependent on the purpose and level of detail of studies. Particularly for the urban area studies, a high spatial resolution is needed to support detailed land use classification. However, visual analysis requires a longer time compared to digital analysis of remote sensing images. Therefore, an image with high spatial resolution and various spectral characteristics becomes a good alternative for urban studies to address the complexity and spatial heterogeneity in an urban area. Vegetation is one of the parameters to make urban environment more attractive which also plays a role as a balancing factor in urban ecology. In urban studies and remote sensing, vegetation is often analyzed in terms of its distribution, species, biomass, and even oxygen content, although problems still occurred in calculating vegetation density due to high building density, accessibility, and the mixture between vegetation and bare land.

High density of vegetation in urban areas is difficult to see nowadays. Although the government has promoted 30% of urban area should be for the green area (Hidayati, 2013), the conversion of urban- green area into built up area are still prominent causing low density of vegetation. Vegetation index is a parameter from remote sensing data which represent the greenish level of vegetation and it can distinguish the reflectance of vegetation with other objects.

Vegetation Indices have been extensively used for climate studies (Kaspersen et al., 2015; Stefanov & Netzbund, 2005; Zhang et al., 2013), vegetation density (T. Liu & Yang, 2013), urban green area (Caroline & Hidayati, 2016; Gago et al., 2013; Kabisch, 2015; T. Liu & Yang, 2013), biomass (Prabhakara et al., 2015), estimation of production (Gitelson et al., 2012; Zhao et al., 2018), and estimation of nitrogen content in vegetation (Kimm & Ryu, 2015; Prabhakara et al., 2015). Vegetation index is a value obtained from a combination of several specific spectral bands from a remote sensing image. The near infrared spectrum, healthy green leaves tend to reflect and transmit electromagnetic energy but only slightly absorb electromagnetic energy. This tendency causes the near-infrared spectrum to be very sensitive to changes in density of broadleaves because a portion of the infrared spectrum energy will be reflected back by the leaf's surfaces beneath it. In the green band, the reflectance values of vegetation will be good. More leaves areas affect the reflectance values of the spectral vegetation due to the increased content of chlorophyll in leaves. The value of vegetation index is obtained from the energy emitted by vegetation

in the remote sensing image to show the life-size and amount of a plant. However, challenges arise when the calculation of the vegetation index is carried out in urban areas. Vegetation becomes scarcer as the green area conversion and urban area with its dynamic characteristics fills up the land with buildings.

Some normalized indices have been calculated using Worldview-2 imagery. The Normalized Difference Bare Soil Index (NDBSI) which involves blue channels and coastal blue; Normalized Difference Water Index (NDWI) which uses green and NIR2 (Sun et al., 2016); and NDVI that uses red and infrared (Weng & Fu, 2014). Another normalized index related to vegetation has also been used by De Benedetto et al., (2013) who calculated NDVI using NIR1 and red, and Normalized Difference Red Edge Index using NIR and Red Edge. Further, index calculation using normalized indices have also been widely used. The use of simple normalized indices allows researchers to explore the role and function of each band of a particular image. Worldview-2 imagery, with the advantages of spatial resolution and spectral resolution, offers researchers the opportunity to explore normalized indices for vegetation density. The development of very high spectral and spatial resolution multispectral imagery such as WorldView-2 (WV-2) has created more opportunities for remote sensing applications especially in urban mapping. This sensor is characterized by very high spatial resolution (2 m) data in eight spectral bands (between 450-1050 nm). The sensor also has panchromatic data at 0.5 m spatial resolution between 450-800nm. This image is completed with coastal blue (400-450 nm), yellow (585-625 nm), red-edge (705-745 nm) and NIR2 (860-1040 nm) bands. Carrying bands of NIR1, NIR2, Red, and Red Edge, Worldview-2 allows the calculation of various indices modifications (Hidayati et al., 2018). This study aims to find the best combination of Normalized Index (NI) of Worldview-2 for estimation of vegetation density in the study area. The best combination was selected based on the mapping accuracy from overall accuracy and kappa coefficients.

2. The Methods

Digital number of Worldview-2 imagery must be converted to radiance values before radiometric correction or other spectral analysis, and before comparison with other sensors or spectral reflections (Digital Globe, 2010). In this study, we used Worldview-2 imagery obtained from the Digital Globe Foundation, with the acquisition date of September 16, 2015. Variation in spectral resolutions in Worldview-2 (Table 1) enables this study to select the best index combination calculated from the eight bands.

Normalized Indices

Vegetation index that is often used is the Normalized Difference Vegetation Index (NDVI) which involves infrared and red wavelengths. The range of values in

Table 1. Spatial and spectral resolutions of Worldview 2.

Bands	Worldview 2
Panchromatic	450 – 800 nm
Spatial resolution	0,46 m
Coastal Blue (CB)	400 – 450 nm
Blue (B)	450 – 510 nm
Green (G)	510 – 580 nm
Yellow (Y)	585 – 625 nm
Red (R)	630 – 690 nm
Red Edge (RE)	705 – 745 nm
NIR-1 (NIR-1)	770 – 895 nm
NIR-2 (NIR-2)	860 – 1040 nm

Source: DigitalGlobe, 2014

this NDVI is -1 to 1 where the value of -1 to 0 means non-vegetation class and range of 0-1 means vegetation class. This value is actually not an absolute value because the threshold value must be adjusted to the distribution of the pixel value itself. The calculation of NDVI in this study involved eight bands in the Worldview-2 image, starting from a coastal-blue combination with blue (NI1), Coastal-blue with green (NI2), to NIR-2 with NIR-1 (Table 2). In detail, the research framework is illustrated in the workflow (Fig.1). The method used in this study is to make normalized index using all bands in the WorldView-2 image. Band combination starts from the combination of Coastal Blue with Blue using the formula:

$$NI = \frac{\text{band 1} - \text{band 2}}{\text{band 1} + \text{band 2}} \quad (1)$$

A total of 56 index combinations were obtained from the normalized index process in the previous process. The second thing to do is to determine the threshold value (Table 3). Index ratios are usually used to classify certain material or features that are determined for differences in certain channel reflectance values. Normalized Index assumes that the probability distribution is symmetrical. This assumption is reasonable and in line with stochastic control theory where interference is often assumed and comes from a Gaussian distribution. Based on this assumption, process variables can be expected to fluctuate or spread according to the data curve and set-point. When a problem appears in the calculation, the set-point cannot be achieved causing this assumption will be violated. This normalized index is used to detect problems related to the magnitude of irregularities at the set-point (Salsbury & Alcalá, 2017). Regarding land use mapping, the normalized index can be used to establish the classification basis by identifying surface reflectance. This identification is needed to distinguish the reflectance between healthy and unhealthy vegetation and between natural and man-made objects. This study involved Worldview-2 images

Table 2. Combinations of Normalized Index for Worldview-2 imagery.

No	Normalized Index	Band Names	No	Normalized Index	Band Names
1	b1b2	CB,B	29	b5b1	R,CB
2	b1b3	CB,G	30	b5b2	R,B
3	b1b4	CB,Y	31	b5b3	R,G
4	b1b5	CB,R	32	b5b4	R,Y
5	b1b6	CB,RE	33	b5b6	R,RE
6	b1b7	CB,NIR-1	34	b5b7	R,NIR-1
7	b1b8	CB,NIR-2	35	b5b8	R,NIR-2
8	b2b1	B,CB	36	b6b1	RE,CB
9	b2b3	B,G	37	b6b2	RE,B
10	b2b4	B,Y	38	b6b3	RE,G
11	b2b5	B,R	39	b6b4	RE,Y
12	b2b6	B,RE	40	b6b5	RE,R
13	b2b7	B,NIR-1	41	b6b7	RE,NIR-1
14	b2b8	B,NIR-2	42	b6b8	RE,NIR-2
15	b3b1	G,CB	43	b7b1	NIR-1,CB
16	b3b2	G,B	44	b7b2	NIR-1,B
17	b3b4	G,Y	45	b7b3	NIR-1,G
18	b3b5	G,R	46	b7b4	NIR-1,Y
19	b3b6	G,RE	47	b7b5	NIR-1,R
20	b3b7	G,NIR-1	48	b7b6	NIR-1,RE
21	b3b8	G,NIR-2	49	b7b8	NIR-1,NIR-2
22	b4b1	Y,CB	50	b8b1	NIR-2,CB
23	b4b2	Y,B	51	b8b2	NIR-2,B
24	b4b3	Y,G	52	b8b3	NIR-2,G
25	b4b5	Y,R	53	b8b4	NIR-2,Y
26	b4b6	Y,RE	54	b8b5	NIR-2,R
27	b4b7	Y,NIR-1	55	b8b6	NIR-2,RE
28	b4b8	Y,NIR-2	56	b8b7	NIR-2,NIR-1

Note: CB = coastal blue band, B=blue band, G = Green band, Y=Yellow band, R = Red band, RE = Red Edge band, NIR1 = NIR-1 band, NIR2 = NIR-2 band.

with eight spectral bands producing 56 combinations of normalized indices (Table 2). The normalized index with the same two bands is however not used in the study, such as the blue-blue bands normalized index or the other.

Threshold Value

This threshold value is used to separate the appearance of vegetation and non-vegetation. The choice of the threshold value must be adjusted to the

characteristics of the region. Variations in land use determine the threshold value used. After the threshold process is obtained, the binary index is done to separate the vegetation area and not the vegetation. The easiest method for segmentation is by using a threshold value. To make segmentation more consistent, the threshold value is determined by the system or software. Knowledge about object shapes, spectral characteristics of image, local-knowledge, and background knowledge about certain land uses are very strong provision for the threshold determination. In general, a good threshold can be chosen if the peak histogram is high, narrow, symmetrical, and can be separated by a deep enough valley (Nenzén & Araújo, 2011; Valentinitich et al., 2012). Thresholding is used to extract surface objects that have the same intensity background value (T value) for each pixel, so each pixel is classified as an object point. Measurement of homogeneous regions is variance where areas with high homogeneity will have low variance values. In this study, we applied the Otsu method for the thresholding. Otsu method selects threshold values by minimizing variance in classes between two groups of pixels which are distinguished by systems/classifications (Chengyang et al., 2012). Otsu does not depend on the probability density function, instead, it assumes a bimodal distribution of the brightness level (grey level). It involves iteration (repetition) through all possible threshold values and calculates the distribution of each pixel at all sides of the threshold. This calculation was to determine a threshold value at the center of the pixel that differs from the pixel values around it. The grey level in thresholding functions is used as a detector to distinguish between desired and unwanted objects (main objects with background objects). After the thresholding is done, the image binarization process is carried out by considering the variation of background intensity and noise.

Field Measurement and Accuracy Test

Accuracy Test is carried out by considering field samples with a total of 250 sample points obtained using the stratified random sampling method. The parameters taken in the field are land use and vegetation area. This field measurement is to ensure the correctness of the type of land use compared to visual analysis. These 12 indices are used to calculate the area of vegetation in the study area. Accuracy test includes sampling design, response design, estimation, and analysis procedures. Selection of a sampling strategy is important including the selection of sampling unit, sampling design, and sample size (Schelin & Sjöstedt-De Luna, 2014). In this study, we used a stratified random sampling (Priebe et al., 2001; Rougier, Puissant et al., 2016; Stehman, Hansen et al., 2011) with a total sample of 250 samples for the field test. After conducting a field test, the calculation of accuracy testing was done based on a pixel-based approach, which is a calculation based on pixel values. In calculating the mapping accuracy matrix, there are several factors that must be considered, namely reference data collection, classification schemes, sampling schemes, spatial autocorrelation, sample size and sample units (D. Liu & Xia, 2010). Congalton (2010) systematically explained the principles and practical considerations in designing and evaluating basic accuracy related to fuzzy logic and multilayer mapping. The kappa coefficient is the overall statistical measure in an error matrix which accounts for matrix errors. Kappa analysis is recognized as a powerful method for analyzing single matrix errors and for comparing differences between various error matrices.

Measurement of the vegetation area used the results of index combination images processed by binarization. The threshold values became the basis to create those index and binary images (Fig.5). This binarization process used five best accuracy combination out of 56

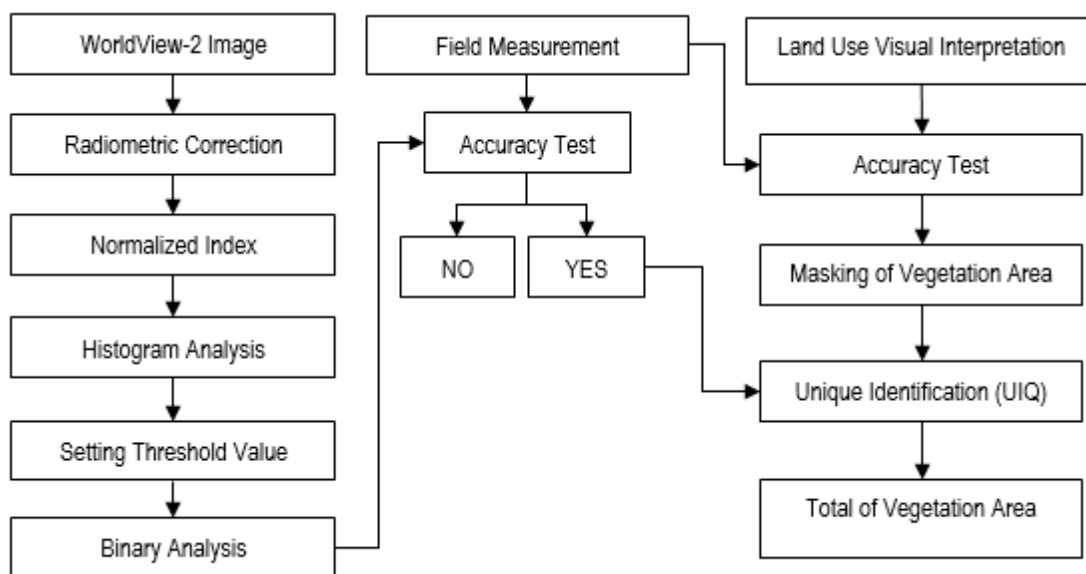


Figure 1. Research flowchart.

index combinations. Accuracy test is used to test the accuracy of the segmentation and vegetation area in visual image analysis. The first accuracy test is done for segmentation accuracy test (threshold result). The results of segmentation were tested for accuracy to determine the accuracy of differences in vegetation and non-vegetation. The second accuracy test was carried out on the results of a visual analysis of land use that was used to test the accuracy of the area of vegetation. Overall accuracy and kappa coefficient were calculated as the accuracy indicators of vegetation and non-vegetation classes. Calculation of vegetation area used Unique Identification (UID) hence the vegetation density of each grid can be measured in detail (Hidayati et al., 2018; Kumar et al., 2012). A total of 756 grids with the size of 50 x 50 was used.

3. Results and Discussion

Vegetation Indices based on Normalized Index

The vegetation index results obtained from the normalized index created (56 combinations). Of the 56 combinations made, 37 combinations were used for the accuracy test process. A total of 19 combinations were not used because they were not good visually and the resulting sprocket value did not represent the results of index normalization. In this study selected 37 combinations for accuracy testing. The result of the normalized index (Fig.2) was used for the reference to make the binary index (Fig.3). This binary index was made to clearly separate the vegetation and non-vegetation classes. The spectral bands of the worldview image are processed to do a normalized index. Normalization index results are used after being selected and adjusted to the research objectives, namely

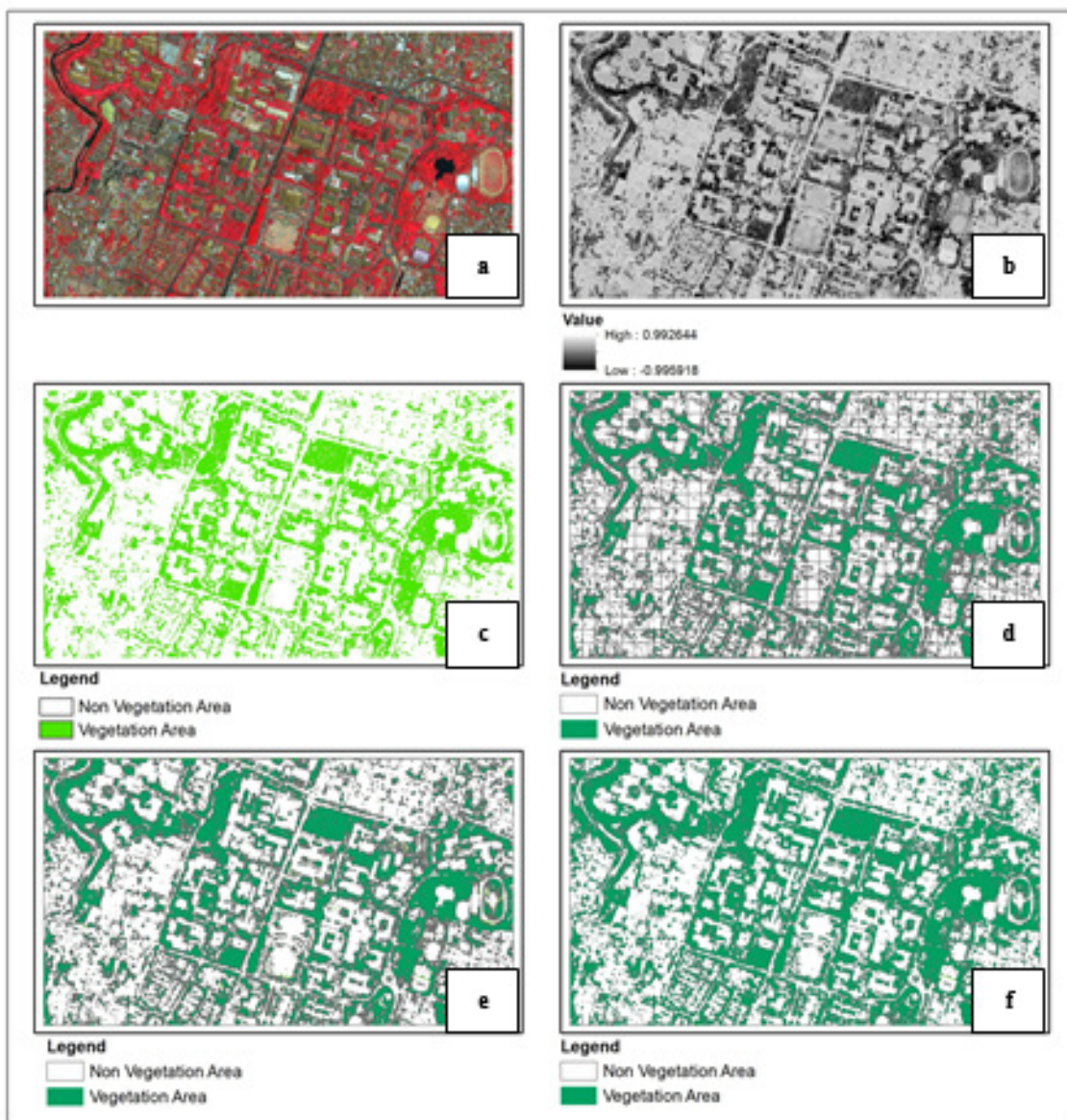


Figure 2. Vegetation indices calculation process. (a) Worldview-2 imagery, (b) Normalized Index, (c) Binary Index, (d) Unique Identification (UID), (e) Result of overlay, (f) Result of generalization.

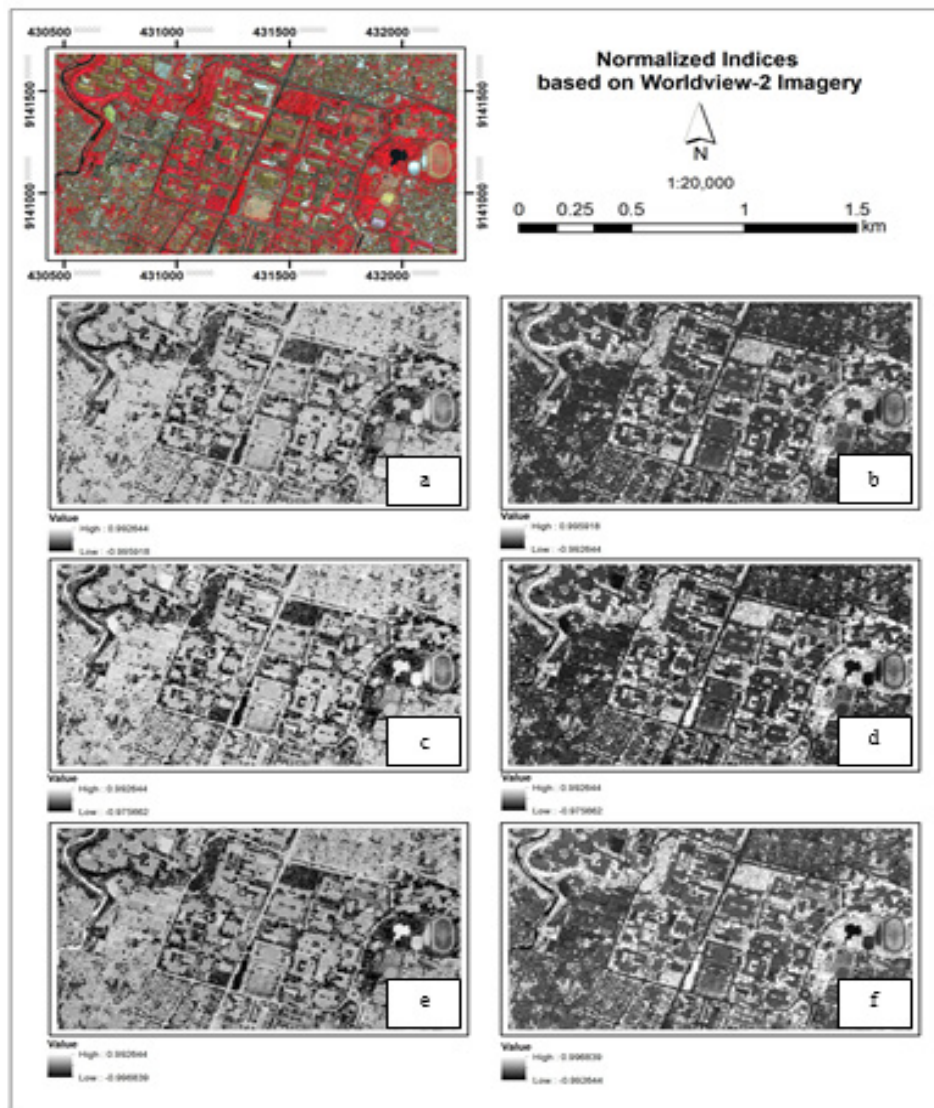


Figure 3. Results of Normalized Index (NI) from Worldview-2 image (a) Worldview-2 image, (b) Combination of NI 65, (c) Combination of NI 75, (d) Combination of NI 85, (e) Combination of NI 56, (f) Combination of NI 57, (g) Combination of NI 58.

those that have a clear visual appearance and can be used spectrally. 56 combinations were carried out normalizing the index in accordance with the formula 1 (Fig.2). From the combination results, a threshold value analysis was carried out with Otsu thresholding. Threshold results that meet the requirements are used for image accuracy testing. The results of this accuracy are related to vegetation and non-vegetation. The image used for the accuracy test is 37 images (Fig.3), but it is accepted and has an accuracy above 85% as many as 12 image combinations. 12 image combinations were carried out by UIQ analysis. The function of this analysis is to obtain the area of vegetation in the research area. Accuracy test is done and adjusted to the results of visual image analysis. The results of visual image analysis also carried out accuracy tests to ensure the correctness of visual image analysis. After obtaining

UIQ results, extraction of vegetation area was carried out to obtain vegetation results in the study area. Visual analysis was used as a baseline for the accuracy of the area of vegetation in the study area. Generalizations are still made to obtain smoother results.

The difference between the spectral response values in NI determines the threshold values for different land uses. First, the study area was identified. Then, the threshold value was determined to classify the type of land use. This threshold determination was based on variations of the existing spectral characteristics and the spectral value of each land use. Determining the threshold values is the most important step in calculating an index since the threshold value will affect the mapping accuracy and precision. After the threshold determination, the binary index was carried out. The process for the NI involved a binary index with

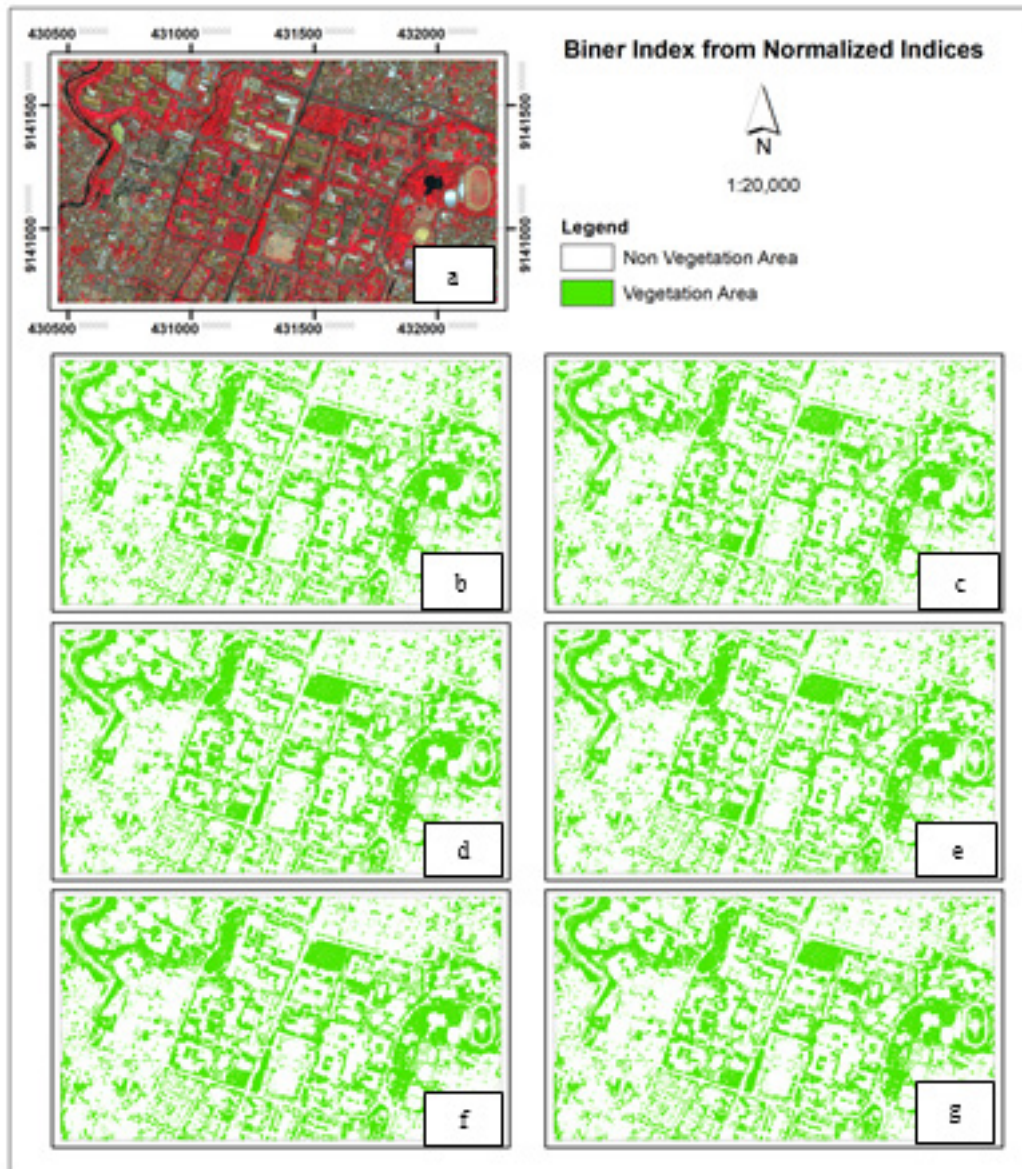


Figure 4. Result of binarization of Worldview-2 image (a) Worldview-2 image, (b) Binary index 65, (c) Binary index 75, (d) Binary index 85, (e) Binary index 56, (f) Binary index 57, (g) Binary index 58.

the value of 1 for vegetation and the value of 0 for non-vegetation area (Fig.4). Each NI was processed based on different threshold values that have been adjusted to the spectral characteristics of each band.

Threshold Value

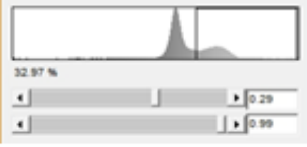

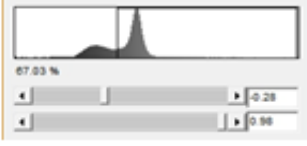



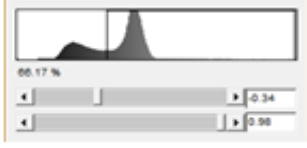



In this study, a total of 56 histograms were made to separate vegetation and non-vegetation objects. The threshold range was not always between -1 to 0 and 0 to 1 but it was adjusted to the characteristics of each reflectance signature or the pixel value. Table 3 shows five threshold values out of 56 thresholds determined by Otsu Thresholding.

Selection of the best accuracy

The best accuracy was selected after all NI accuracy tests using 250 field samples. We selected

five best accuracies from 56 combinations (Table 4). We found that the bands involved in the five best accuracies were red, red-edge, NIR-1 and NIR-2 from the band combinations of NI40, NI33, NI47, NI34 and NI54. The characteristics of the red wavelength in the WorldView-2 image (630-690 nm) which focuses on the absorption of chlorophyll in healthy plants, is one of the bands that is very sensitive to vegetation and is used for the classification of bare soils, roads, and geological phenomena. Furthermore, red-edge wavelength (705-745 nm) which has a high reflectance of vegetation, is usually used to classify and measure the health of vegetation. NIR-1 is very effective for moisture content estimation and biomass measurement and is very effective for differentiating water with vegetation, identifying types of vegetation, and distinguishing vegetation from soil.

Table 3. Threshold values for five combinations of Normalized Index (NI).

NI	Threshold	Threshold Diagram	Image Result
b6b5	0.29		
b5b6	-0.28		
b7b5	0.35		
b5b7	-0.34		
b8b5	0.29		

Note: NI is normalized index formula.

Table 4. Best accuracy values from band combinations of Normalized Index (NI).

Band combinations	Kappa Coefficient	Overall Accuracy
b6b5	0.98	95.84%
b5b6	0.98	94.62%
b7b5	0.98	94.38%
b5b7	0.97	93.13%
b8b5	0.97	91.81%

The accuracy received is 85% or higher. Of the 56 combinations made, 37 index combinations were accepted, and 28 index combinations were rejected. 19 this index combination is rejected because the vegetation distribution results are uneven, the index value does not meet the established procedure, that is, visually cannot be used because what appears to be only a few pixels or spectrally has inappropriate spectral variance, and too many vegetation areas were overestimates. Of the 37 combinations of indexes received, 12 of them have accuracy values above 85%.

Vegetation Area Measurement

The amount of vegetation in the field is needed to find out the number of urban green areas. Visual analysis is one analysis that is often used to detect green and non-green urban open spaces. The weakness of visual analysis is that it takes a long time to digitize and manipulate data. This study uses an index approach to calculate the number of urban green areas by normalized index. Field data is used to accuracy test of vegetation or not vegetation. The results of visual analysis are used to test the accuracy of extensive vegetation (Fig.5).

Finally, calculation of accuracy and precision for vegetation density were compared with the results of visual analysis of Worldview-2 images. The visual analysis resulted in area of 62.64 m² for vegetation class. The results of the study (table 5) showed that red-edge and red band combinations gets an accuracy of 90.61% with area differences with visual analysis of 5.88 m². The best result is NIR2 and red which has an accuracy test of 96.29% with an estimated vegetation area lower than visual analysis of 2.32 m². The combination of NIR1 and red has quite high accuracy, which is 94.53% with an underestimate of 3.43 m² of vegetation area. From the results of the estimation of the vegetation area

all results show that there is an underestimate from the results of visual analysis.

All band combinations which involves four bands (red, red-edge, NIR-1, and NIR 2 bands) produced the best accuracy because of their sensitivity to vegetation. Surprisingly, the combination of red-edge with red bands produced a high accuracy. Yellow band that is combined with red, red-edge, NIR1 and NIR2 bands also generated a good result. We found that the yellow band is good to separate bare land and vegetation areas. The red-edge band produced a good combination for vegetation, thus it can be applied to map the health of plants as it represents the reflectance of chlorophyll. In this study, we included the red-edge band for the index combination considering the vegetation type in urban area. Urban vegetations are usually scattered in park, urban forest, and river riparian area, thus the red-edge band will be useful as it can highlight the photosynthetic process in healthy vegetation.

Obtaining the best accuracy is the main objective in studies related to mapping from remote sensing data. High accuracy values are influenced by basic knowledge, sufficient field data, methods, and heterogeneous samples to represent actual data (Lizarazo, 2014). In this study, the accuracy was influenced by the selection of band combinations considering the characteristics of image band and object. Despite the good accuracy, the process of calculating band combinations was quite exhaustive. The process involved making normalized indices to produce band combinations, selecting the threshold values, making a binary index for vegetation and non-vegetation classification, testing the accuracy based on pixel values, and calculating vegetation density in WorldView-2 imagery.

The accuracy values were tested from 250 field samples. From the accuracy values, it was found that the combination of bands that use NIR-2, NIR-1, red, and red-edge produced the highest accuracy with kappa coefficient of 0.96-0.98 and overall accuracy of 90.68% - 95.84%. When the yellow band was used in combination with NIR-1, NIR-2, and red-edge, the kappa coefficient was still 0.93-0.96, but the overall accuracy decreased

by 85.37% -90.24%. In addition, the inclusion of green and blue band into the combination of red-edge, red, NIR-1, and NIR-2 gave a lower accuracy ranging from 0.77 - 0.84 and overall accuracy ranging from 59.40% - 65.91%. The combination of NIR-1 and red band had a high accuracy of 94.38% with kappa coefficients of 0.98. The surprising result was from the combination of red-edge and red that produced an accuracy of 95.84% with a kappa coefficients of 0.98. These findings show that the band combinations that involve red, red-edge, NIR-1, and NIR-2 band remained to be the best band combinations.



Figure 5. Comparison of vegetation area values from two methods (a) Image visual analysis and (b) Normalized Index calculation.

Table 5. Result of the best accuracy.

Combination Band	Land Use	Vegetation Area	Percentage of Vegetation Area	Underestimate (m2)	Overall Accuracy
65	Non-Vegetation	119.50	67.80	-5.88	90.61
	Vegetation	56.75	32.20		
56	Non-Vegetation	117.72	66.79	-4.10	93.45
	Vegetation	58.53	33.21		
75	Non-Vegetation	117.04	66.41	-3.43	93.45
	Vegetation	59.21	33.59		
85	Non-Vegetation	115.94	65.78	-2.32	96.29
	Vegetation	60.31	34.22		

Testing of vegetation area accuracy was also carried out comparing the area from the normalized index with visual analysis. It was found that the combination using NIR-2 and red produced the best accuracy and precision with an accuracy of 96.29% (area of 2.32 m² was underestimated) in comparison to the visually extracted area. This means that vegetation area obtained from the index gave a lower value when compared to visual analysis. The second best accuracy value was obtained from the combination of NIR-1 and red bands (accuracy of 94.53%) with a shifted area of 3.43 m² (Table 5).

4. Conclusions

Satellite imagery with visible wavelengths has limitations in spectral range characteristics. However, WorldView-2 imagery provides additional spectral characteristics that can be used for automatic exploration and extraction of various image indices. This study aims to determine the best combination of indices for estimating vegetation density in some urban areas in Yogyakarta. From a total of 56 index combination, our results shows that the combinations involving NIR1, NIR2, Red, and red-edge have better accuracy than other combinations. We found that the combination of red and red-edge band gave the best accuracy from the binary test to classify vegetation or non-vegetation. Involvement of yellow band also affected the accuracy as it can help in identifying healthy and woody vegetation. In this study, the red-edge performance was sufficiently taken into account.

The selection of threshold values is also essential for the accuracy. A value less than 1.0 does not necessarily indicate that the pixel is not vegetation, but the selection of the threshold value needs to be adjusted to the distribution of pixel values in the image. Different band combinations will lead to a difference in pixel value distribution which directly impact on the threshold value selection. The UID process of a grid was chosen to calculate vegetation density. Accuracy testing of vegetation area was also carried out and compared with the results of the visual analysis. We concluded that the combination of NIR2 and red band gave the highest accuracy accounted 94.38% of the visually calculated area. The choice of study location also affected the combination of bands used. For the next studies, we suggest that the analysis can be divided into two seasons, dry and rainy season to maximize the performance of yellow band as shown in this study that yellow band is good to separate bare land and vegetation areas.

Acknowledgments

The authors thank the Digital Globe Foundation for giving the Worldview-2 imagery as a main data of this research. Thanks to DIKTI for giving Doctoral research grants to support research funding. The authors also thank the Dean, Vice Deans, and all lecturers in Faculty of Geography.

References

- Caroline, A. H., & Hidayati, I. N. (2016). Pemanfaatan Citra Quickbird dan SIG untuk Pemetaan Tingkat Kenyamanan Permukiman di Kecamatan Semarang Barat dan Kecamatan Semarang Utara. *Majalah Geografi Indonesia*, 30(1), 1–8.
- Chengyang, W., Shixiong, H., Wenjing, S., & Wei, C. (2012). Fractal dimension of coal particles and their CH₄ adsorption. *International Journal of Mining Science and Technology*, 22(6), 855–858. <https://doi.org/10.1016/j.ijmst.2012.11.003>
- Congalton, R. G. (2010). Remote Sensing: An Overview. *GIScience & Remote Sensing*, 47(4), 443–459. <https://doi.org/10.2747/1548-1603.47.4.443>
- De Benedetto, D., Castrignanò, A., Rinaldi, M., Ruggieri, S., Santoro, F., Figorito, B., ... Tamborrino, R. (2013). An approach for delineating homogeneous zones by using multi-sensor data. *Geoderma*, 199, 117–127. <https://doi.org/10.1016/j.geoderma.2012.08.028>
- Digital Globe. (2010). Radiometric Use of WorldView-2 Imagery Technical Note 1 WorldView-2 Instrument Description, (November), 1–17.
- Duro, D. C., Franklin, S. E., & Dubé, M. G. (2012). A comparison of pixel-based and object-based image analysis with selected machine learning algorithms for the classification of agricultural landscapes using SPOT-5 HRG imagery. *Remote Sensing of Environment*, 118, 259–272. <https://doi.org/10.1016/j.rse.2011.11.020>
- Gago, E. J., Roldan, J., Pacheco-Torres, R., & Ordóñez, J. (2013). The city and urban heat islands: A review of strategies to mitigate adverse effects. *Renewable and Sustainable Energy Reviews*, 25, 749–758. <https://doi.org/10.1016/j.rser.2013.05.057>
- Gitelson, A. A., Peng, Y., Masek, J. G., Rundquist, D. C., Verma, S., Suyker, A., ... Meyers, T. (2012). Remote estimation of crop gross primary production with Landsat data. *Remote Sensing of Environment*, 121, 404–414. <https://doi.org/10.1016/j.rse.2012.02.017>
- Hidayati, I. N. (2013). Ekstraksi Data Indeks Vegetasi untuk Evaluasi Ruang Terbuka Hijau berdasarkan Citra ALOS di Kecamatan Ngaglik Kabupaten Sleman Yogyakarta. *Agroteknologi*, 3(2), 27–34.
- Hidayati, I. N., Suharyadi, R., & Danoedoro, P. (2018). Kombinasi Indeks Citra untuk Analisis Lahan Terbangun dan Vegetasi Perkotaan. *Majalah Geografi Indonesia*, 32(1), 24–32.
- Kabisch, N. (2015). Ecosystem service implementation and governance challenges in urban green space planning-The case of Berlin, Germany. *Land Use Policy*, 42, 557–567. <https://doi.org/10.1016/j.landusepol.2014.09.005>
- Kaspersen, P. S., Fensholt, R., & Drews, M. (2015). Using Landsat vegetation indices to estimate impervious surface fractions for European cities. *Remote Sensing*, 7(6), 8224–8249. <https://doi.org/10.3390/rs70608224>
- Kimm, H., & Ryu, Y. (2015). Seasonal variations in

- photosynthetic parameters and leaf area index in an urban park. *Urban Forestry and Urban Greening*, 14(4), 1059–1067. <https://doi.org/10.1016/j.ufug.2015.10.003>
- Kumar, A., Pandey, A. C., & Jeyaseelan, A. T. (2012). Built-up and vegetation extraction and density mapping using WorldView-II. *Geocarto International*, 27(7), 557–568. <https://doi.org/10.1080/10106049.2012.657695>
- Liu, D., & Xia, F. (2010). Assessing object-based classification: Advantages and limitations. *Remote Sensing Letters*, 1(4), 187–194. <https://doi.org/10.1080/01431161003743173>
- Liu, T., & Yang, X. (2013). Mapping vegetation in an urban area with stratified classification and multiple endmember spectral mixture analysis. *Remote Sensing of Environment*, 133, 251–264. <https://doi.org/10.1016/j.rse.2013.02.020>
- Lizarazo, I. (2014). Accuracy assessment of object-based image classification: another STEP. *International Journal of Remote Sensing*, 35(16), 6135–6156. <https://doi.org/10.1080/01431161.2014.943328>
- Nenzén, H. K., & Araújo, M. B. (2011). Choice of threshold alters projections of species range shifts under climate change. *Ecological Modelling*, 222(18), 3346–3354. <https://doi.org/10.1016/j.ecolmodel.2011.07.011>
- Prabhakara, K., Dean Hively, W., & McCarty, G. W. (2015). Evaluating the relationship between biomass, percent groundcover and remote sensing indices across six winter cover crop fields in Maryland, United States. *International Journal of Applied Earth Observation and Geoinformation*, 39, 88–102. <https://doi.org/10.1016/j.jag.2015.03.002>
- Priebe, C. E., Naiman, D. Q., & Cope, L. M. (2001). Importance sampling for spatial scan analysis: Computing scan statistic p-values for marked point processes. *Computational Statistics and Data Analysis*, 35(4), 475–485. [https://doi.org/10.1016/S0167-9473\(00\)00017-7](https://doi.org/10.1016/S0167-9473(00)00017-7)
- Rougier, S., Puissant, A., Stumpf, A., & Lachiche, N. (2016). Comparison of sampling strategies for object-based classification of urban vegetation from Very High Resolution satellite images. *International Journal of Applied Earth Observation and Geoinformation*, 51, 60–73. <https://doi.org/10.1016/j.jag.2016.04.005>
- Roy, P. S., Behera, M. D., Murthy, M. S. R., Roy, A., Singh, S., Kushwaha, S. P. S., ... Ramachandran, R. M. (2015). New vegetation type map of India prepared using satellite remote sensing: Comparison with global vegetation maps and utilities. *International Journal of Applied Earth Observation and Geoinformation*, 39, 142–159. <https://doi.org/10.1016/j.jag.2015.03.003>
- Salsbury, T. I., & Alcalá, C. F. (2017). A method for setpoint alarming using a normalized index. *Control Engineering Practice*, 60(May 2016), 1–6. <https://doi.org/10.1016/j.conengprac.2016.12.002>
- Schelin, L., & Sjöstedt-De Luna, S. (2014). Spatial prediction in the presence of left-censoring. *Computational Statistics and Data Analysis*, 74, 125–141. <https://doi.org/10.1016/j.csda.2014.01.004>
- Stefanov, W. L., & Netzband, M. (2005). Assessment of ASTER land cover and MODIS NDVI data at multiple scales for ecological characterization of an arid urban center. *Remote Sensing of Environment*, 99(1–2), 31–43. <https://doi.org/10.1016/j.rse.2005.04.024>
- Stehman, S. V., Hansen, M. C., Broich, M., & Potapov, P. V. (2011). Adapting a global stratified random sample for regional estimation of forest cover change derived from satellite imagery. *Remote Sensing of Environment*, 115(2), 650–658. <https://doi.org/10.1016/j.rse.2010.10.009>
- Sun, G., Chen, X., Jia, X., Yao, Y., & Wang, Z. (2016). Combinational Build-Up Index (CBI) for Effective Impervious Surface Mapping in Urban Areas. *IEEE Journal of Selected Topics in Applied Earth Observations and Remote Sensing*, 9(5), 2081–2092. <https://doi.org/10.1109/JSTARS.2015.2478914>
- Valentinitsch, A., Patsch, J. M., Deutschmann, J., Schueller-Weidekamm, C., Resch, H., Kainberger, F., & Langs, G. (2012). Automated threshold-independent cortex segmentation by 3D-texture analysis of HR-pQCT scans. *Bone*, 51(3), 480–487. <https://doi.org/10.1016/j.bone.2012.06.005>
- Weng, Q., & Fu, P. (2014). Modeling annual parameters of clear-sky land surface temperature variations and evaluating the impact of cloud cover using time series of Landsat TIR data. *Remote Sensing of Environment*, 140, 267–278. <https://doi.org/10.1016/j.rse.2013.09.002>
- Zhang, Y., Gao, J., Liu, L., Wang, Z., Ding, M., & Yang, X. (2013). NDVI-based vegetation changes and their responses to climate change from 1982 to 2011: A case study in the Koshi River Basin in the middle Himalayas. *Global and Planetary Change*, 108, 139–148. <https://doi.org/10.1016/j.gloplacha.2013.06.012>
- Zhao, B., Duan, A., Ata-Ul-Karim, S. T., Liu, Z., Chen, Z., Gong, Z., ... Ning, D. (2018). Exploring new spectral bands and vegetation indices for estimating nitrogen nutrition index of summer maize. *European Journal of Agronomy*, 93(December 2017), 113–125. <https://doi.org/10.1016/j.eja.2017.12.006>